

SUPER AGB – AGB EVOLUTION AND THE CHEMICAL INVENTORY IN NGC 2419

PAOLO VENTURA

INAF – Osservatorio Astronomico di Roma, via Frascati 33, I-00040 Monteporzio, Italy

FRANCESCA D’ANTONA

INAF – Osservatorio Astronomico di Roma, via Frascati 33, I-00040 Monteporzio. Italy

MARCELLA DI CRISCIENZO

INAF- Osservatorio Astronomico di Capodimonte, Salita Moiariello 16, I-80131 Napoli (Italy)

ROBERTA CARINI

INAF- Osservatorio Astronomico di Roma, via Frascati 33, I-00040 Monteporzio, Italy

ANNIBALE D’ERCOLE

INAF- Osservatorio Astronomico di Bologna, via Ranzani 1, I-40127 Bologna (Italy)

ENRICO VESPERINI

Department of Astronomy, Indiana University, Bloomington, USA

Draft version February 26, 2024

ABSTRACT

We follow the scenario of formation of second generation stars in globular clusters by matter processed by hot bottom burning (HBB) in massive asymptotic giant branch (AGB) stars and super-AGB stars (SAGB). In the cluster NGC 2419 we assume the presence of an extreme population directly formed from the AGB and SAGB ejecta, so we can directly compare the yields for a metallicity $Z=0.0003$ with the chemical inventory of the cluster NGC 2419.

At such a low metallicity, the HBB temperatures (well above 10^8K) allow a very advanced nucleosynthesis. Masses $\sim 6 M_{\odot}$ deplete Mg and synthesize Si, going beyond Al, so this latter element results only moderately enhanced; sodium can not be enhanced. The models are consistent with the observations, although the predicted Mg depletion is not as strong as in the observed stars. We predict that the oxygen abundance must be depleted by a huge factor (>50) in the Mg-poor stars. The HBB temperatures are close to the region where other p-capture reactions on heavier nuclei become possible. We show that high potassium abundance found in Mg-poor stars can be achieved during HBB, by p-captures on the argon nuclei, if the relevant cross section(s) are larger than listed in the literature or if the HBB temperature is higher. Finally, we speculate that some calcium production is occurring owing to proton capture on potassium. We emphasize the importance of a strong effort to measure a larger sample of abundances in this cluster.

Subject headings: stars: AGB and post-AGB

1. INTRODUCTION

Photometric and spectroscopic analysis of Globular Cluster (hereafter GC) stars in the last decades have changed the traditional framework describing the stellar content of these systems: it is now clear that most GCs harbour multiple stellar populations, differing in their original chemistry and characterized by a spread in light elements such as aluminium, sodium, oxygen and magnesium (Gratton et al. 2012, and references therein). These results were reinforced by high-quality photometric data, showing that some GCs harbour multiple main sequences, that can be interpreted by invoking the presence of a helium-enriched population (Norris 2004; D’Antona et al. 2005; Piotto et al. 2007; Milone et al. 2012). This finding is in agreement with the suggestion

that helium could be the second parameter traditionally invoked to account for the anomalous shape of the Horizontal Branch (HB) of some GCs (D’Antona et al. 2002; Caloi & D’Antona 2005).

The above results indicate that the stars with anomalous chemistry were born from matter contaminated by advanced p-capture nucleosynthesis, exposed to temperatures sufficiently large (exceeding $\sim 100\text{ MK}$) to activate the CNO, Ne-Na and Mg-Al nuclear channels (Prantzos et al. 2007). Pollution by ejecta of rapidly rotating massive stars (Decressin et al. 2007a,b), massive binary stars (De Mink et al. 2009), or intermediate mass Asymptotic Giant Branch (AGB) and Super Asymptotic Giant Branch (SAGB)¹ stars

paolo.ventura@oa-roma.inaf.it

¹ SAGB stars are the stars that ignite carbon in conditions of partial degeneracy, form an O-Ne core, and then evolve through

(Cottrell & Da Costa 1981; Ventura et al. 2001) are among the scenarios suggested in the literature. In this work, we follow the hydro-dynamical model for the formation of multiple populations by D’Ercole et al. (2008) and focus on the hypothesis that AGB and SAGB stars, via the strong mass loss at low velocity experienced during their post core Helium burning evolution, produced the polluted material, from which the new stars formed.

Notice that Mg depletion, which is an important signature of the extreme anomalies we will be dealing with, is a severe constraint on the scenarios, as it can not be found in the ejecta of massive stars (Decressin et al. 2007a), nor of massive binaries, subject to similar nucleosynthesis limitations. Only SAGB models with non extreme mass loss rates can predict it (Siess 2010) or massive AGB models with efficient convection (see Ventura et al. 2012). We point out that modelling of AGB and SAGB evolution is subject to considerable uncertainty concerning the efficiency of the hot bottom burning (HBB) and of the third dredge up. Consequently, the AGB–SAGB scenario can explain the chemical patterns in GCs only for those model providing compatible yields. Adoption of an efficient convection (see the discussion in Ventura & D’Antona 2005) provides both reasonable sodium yields and oxygen depletion (plus some Mg depletion at low metallicity), while models with low efficiency of convection and strong dredge up (Karakas & Lattanzio 2003; Karakas 2010; Herwig 2004; Stancliffe et al. 2004) are at variance with AGB–SAGB scenario (Fenner et al. 2004).²

D’Ercole et al. (2010, 2012) showed that the abundance patterns observed can be reproduced provided that the star formation of the second generation (SG) starts immediately after the epoch of the SNII explosions, and is limited to the first ~ 100 Myr, thus involving only stars of mass $M \geq 5M_{\odot}$. The spread observed in the O–Na and Mg–Al planes can be explained by dilution of gas ejected by AGBs with pristine gas present in the cluster. Of extreme interest is the case of massive GCs, where conditions occur for the early formation of a stellar population directly from the winds of SAGBs, with no dilution: these stars are characterized by a strong helium enhancement ($Y \gtrsim 0.35$), and populate the blue MS and the blue tail of the HB of their host clusters. D’Ercole et al. (2012) showed that the SAGB yields are a very important ingredient of the models, for clusters of intermediate metallicity ($[\text{Fe}/\text{H}] \sim -1.5$, i.e. $Z=10^{-3}$). Here we extend our study of the yields from massive AGBs and SAGB stars to the much lower metallicity of $Z=3 \times 10^{-4}$. This metallicity roughly corresponds to $[\text{Fe}/\text{H}] \sim -2$, the iron content of NGC 2419. This cluster is characterized by a HB hosting a blue, faint population, clearly detached from the main component (Ripepi et al. 2007), that can be explained only by invoking a stellar component greatly enriched in helium (Di Criscienzo et al. 2011a). Thus, according to the model by D’Ercole et al. (2008), these stars should be born directly from the ejecta of SAGB and from the most massive AGB stars. Consequently, the

yields computed here should be directly relevant to the chemical composition of the anomalous stars in this clusters. The formation of the SG can be different in other very low metallicity clusters such as M 15 (Snedden et al. 1997), showing non-extreme HB morphology, so here we concentrate on the comparison with NGC 2419 only, and compare our yields to the abundances of O, Na, Mg, Al, Si and K recently made available by Cohen & Kirby (2012) and Mucciarelli et al. (2012).

We further explore the possibility that the bimodal potassium abundances recently discovered by Mucciarelli et al. (2012) in NGC 2419 are a signature of the production of potassium by proton capture on the argon nuclei in the same HBB environment that produces the other abundance anomalies. This can be a powerful indication that the massive AGB/SAGB scenario is indeed operating for the formation of multiple populations.

2. YIELDS FROM AGB AND SAGB STARS

The yields from massive AGB stars of interest in this work are determined by Hot Bottom Burning (HBB), i.e. an advanced, p-capture nucleosynthesis active at the bottom of the convective envelope (Blöcker & Schönberner 1991). Ventura & D’Antona (2005) showed that use of the Full Spectrum of Turbulence (FST, Canuto & Mazzitelli 1991) model for turbulent convection, coupled with the treatment of mass loss by Blöcker (1995), leads easily to HBB conditions for all stars with initial mass $M > 4M_{\odot}$.

Here we present the yields of AGB and SAGB models experiencing HBB for $Z=3 \times 10^{-4}$, $[\alpha/\text{Fe}]=+0.4$, and put into evidence the difference with the $Z=10^{-3}$ models discussed in Ventura & D’Antona (2009, 2011). A detailed discussion of these models will be presented in a forthcoming paper. To allow a more direct comparison with the observations, we show for the i -th species the quantity $[i/\text{Fe}]=\log(X_i/X_{\text{Fe}}) - \log(X_i/X_{\text{Fe}})_{\odot}$.

2.1. Oxygen and Sodium

The degree of the HBB experienced can be deduced by the extent of the oxygen depletion: among all the elements considered, oxygen is the only one whose nuclear activity is a pure destruction process, differently from sodium and aluminium, for which both creation and destruction channels are active, and magnesium, whose nucleosynthesis is complicated by the distribution of the overall magnesium content among the three isotopes (Ventura et al. 2012). In the bottom-right panel of Fig. 1 we show the typical O–Na pattern for the models from 4 to $7.5M_{\odot}$. Similar to the $Z=10^{-3}$ case, the degree of the p-capture nucleosynthesis does not increase monotonically with mass and reaches a maximum around the threshold of $\sim 6M_{\odot}$ ³ separating the AGB from the SAGB regime. The reason (see discussion in Ventura & D’Antona 2011) is in the high mass loss rate of SAGBs, which consumes the envelope before a very advanced nucleosynthesis is experienced. In the

thermal pulses and mass loss like AGB stars (e.g. Siess 2010).

² Lately, Karakas et al. (2012) and Lugaro et al. (2012) are computing models with more efficient convection, that should be able to provide yields closer to the requirements of the GC chemical patterns.

³ Note that this mass, as also the upper limit of $7.5\text{--}8M_{\odot}$ above which SNII explosion occurs, are dependent on the assumed overshoot from the convective core during the core H-burning phase. In this work we used a moderate extra-mixing; if no overshoot was considered, the range of masses involved would shift $1\text{--}5\text{--}2M_{\odot}$ upwards.

panel we note the straight correlation between the oxygen and sodium content of the ejecta. The sodium yields are positive due to the initial phase of sodium synthesis via proton capture onto ^{22}Ne , whereas the correlation is due to simultaneous destruction of oxygen and sodium once the temperature at which the nucleosynthesis occurs exceeds $\sim 80\text{MK}$. The maximum depletion in the surface oxygen reaches $[\text{O}/\text{Fe}] \sim -1.2$ dex at $Z = 3 \times 10^{-4}$, while it was limited to ~ -0.8 dex at $Z = 10^{-3}$ (Ventura & D’Antona 2009, 2011). This is a direct consequence of the increasing temperatures at which the bottom of the surface convective zone is exposed for models of decreasing metallicity. Notice that in the models with maximum oxygen depletion *there can not be any sodium enhancement*.

To illustrate the dependence of the results on the mass loss treatment, and to compare our results with the investigation by Siess (2010), based on smaller rates of mass loss in the high mass domain, we show, for the $6 M_{\odot}$ and $7 M_{\odot}$ models, the results obtained by reducing the mass loss rate to 1/4: thanks to the longer time spent in the HBB phase, oxygen depletion reaches -1.7 dex for the $6 M_{\odot}$, while sodium is not touched in a significant way. A larger O depletion (and further Na depletion) are also found in the $7 M_{\odot}$ evolution. Sodium remains quite large, $[\text{Na}/\text{Fe}] > +0.3$, only in the mass range $7.2\text{--}7.5 M_{\odot}$.

2.2. Magnesium, Aluminium and Silicon

The bottom-left panel of Fig. 1 shows the magnesium and aluminium content of the ejecta. Although the behavior of the total magnesium is complicated by the equilibria of the various p-capture reactions involving the three isotopes, low metallicity models can achieve a magnesium destruction larger than that of $Z = 10^{-3}$ models, with the equilibria among the various species shifted towards heavier elements. Models of mass $M > 5 M_{\odot}$, where the magnesium is most heavily destroyed, show up isotopic ratios $^{25}\text{Mg}/^{24}\text{Mg} \sim 10\text{--}30$ and $^{26}\text{Mg}/^{24}\text{Mg} \sim 1$. The greater magnesium depletion is not associated with a larger aluminium synthesis, because at large temperatures this latter element reaches an asymptotic value of $[\text{Al}/\text{Fe}] \sim +1 - +1.1$ dex, at which a balance is reached between the production and destruction channels. Models showing the strongest depletion of magnesium show an increase of $+0.2$ dex in the silicon abundance (top-left panel). Reducing the mass loss rate to 1/4, the Mg depletion in the $6 M_{\odot}$ increases by -0.1 dex, and Silicon production increases by $+0.1$ dex. In addition, also aluminium decreases. A smaller but similar effect is obtained by following the $7 M_{\odot}$ evolution with reduced mass loss.

2.3. Helium

The models associated to the self-enrichment mechanism, with masses exceeding $\sim 5 M_{\odot}$, eject great quantities of helium in the intra-cluster medium, as a consequence of the second dredge-up, occurring after the core He-burning phase (Ventura et al. 2002; Pumo et al. 2008). We find a helium mass fraction $Y \sim 0.35\text{--}0.37$, for masses $M \geq 5 M_{\odot}$.

3. COMPARISON WITH THE CHEMICAL INVENTORY OF NGC 2419

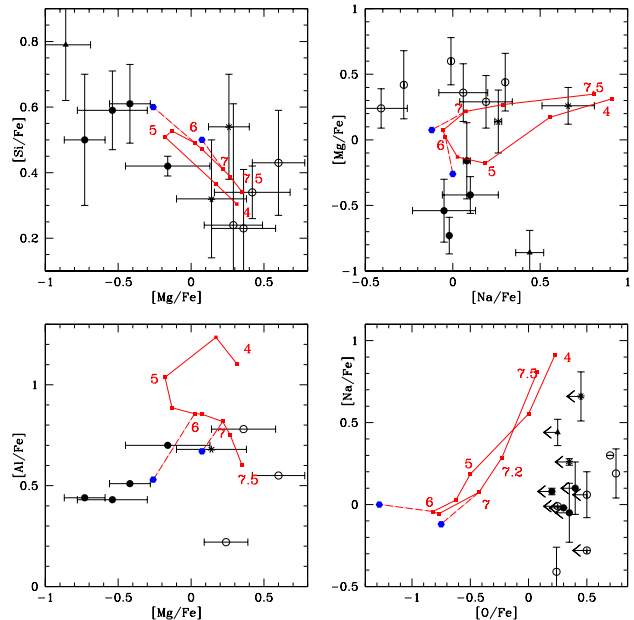


FIG. 1.— Chemical abundances of 13 giants in NGC 2419 (Cohen & Kirby, 2012). In the right-bottom panel, for stars with no abundance determination for oxygen, its upper limit is arbitrarily located in the range $[\text{O}/\text{Fe}] = 0.25\text{--}0.5$ in order to show more clearly the sodium abundance. The error bars (where provided) are the standard deviations listed in Cohen & Kirby 2012. The data are divided into black dots (Mg-poor giants) and open dots (Mg-normal giants). The open dots should represent the first generation stars, having typical α -rich, Na-normal chemical composition. The peculiar giant Mg-poor and Na-rich is shown as a triangle, the two asterisks denote giants with normal Mg and relatively large Na. Black dots, black triangles and asterisks should be compared with the theoretical yields for $Z=3 \times 10^{-4}$, plotted as red squares with the corresponding mass labelled. The two (blue) hexagons are the yields of 6 and $7 M_{\odot}$, when the evolution is computed with mass loss rate reduced to 1/4 of the standard rate.

The large distance of NGC 2419 (87.5 ± 3.38 Kpc from the Sun, Di Criscienzo et al. (2011b)) has precluded an extensive abundance analysis of its stars. However, some fundamental properties have emerged from the work of Cohen et al. (2010, 2011) and Cohen & Kirby (2012), showing the absence of a spread in iron, indicating that the system evolved like a typical GC. Cohen & Kirby (2012) provide abundances for a total of 13 giants, showing the presence of stars with very low Mg abundances, and confirm recent additional data by Mucciarelli et al. (2012) showing an interesting anticorrelation Mg-K. Fig. 1 adds the Cohen & Kirby (2012) data to the theoretical patterns. Cohen & Kirby (2012) noticed that the extreme Mg depletion of some stars did not correspond to a large increase in the Al abundance. Our models however show that the stronger is Mg burning, the more moderate the Al abundance tends to be, as nucleosynthesis proceeds towards nuclei of larger atomic number, with Si production. This is shown clearly by comparing the standard models to those with reduced mass loss, where the time to proceed to more advanced nucleosynthesis is longer, and the Al yields are in the range shown by the Mg-poor giants.

In the panels of Fig. 1 we subdivide Cohen & Kirby data into two main groups: Mg-poor (black dots) and Mg-rich (open dots) giants. We also point out three

possibly “peculiar” giants with moderately large sodium: two giants are shown as asterisks, while a third (S1673 in Cohen & Kirby), very Mg-poor, is shown as a triangle.

First of all, we notice that the oxygen abundances are determined only in a few stars having large abundances. We draw the upper limits in the panel O–Na at arbitrary locations $[O/Fe]=0.25-0.5$ to avoid superposition of the points. In this way we show that the sodium variation encompasses almost 1 dex, but most points cluster at low $[Na/Fe] \lesssim 0.3$. The Mg-depleted giants *also show low sodium* (top-right panel): these data are compatible with our models showing the strongest HBB processing ($5-6 M_{\odot}$). S1673 (shown as a triangle) is an exception.

The open points have normal O, Na and Mg, and thus should be plain “first generation” stars; of the two giants denoted as asterisks, one is Mg-normal, Si-normal, so it is probably an FG star. The other giant (S1305) is very Na-rich ($[Na/Fe]=0.66\pm0.15$) and also Si-rich, but not Mg-poor: we tentatively suggest that it is an SG star formed by SAGB ejecta in the $7.2-7.5 M_{\odot}$ range, stars that had not enough time to deplete Mg too much, but were able to increase Si.

Although the data available are very limited, the observations currently available suggest that the second generation of NGC 2419, identified by Di Criscienzo et al. (2011a) with the blue hook stars can be directly formed from the SAGB – massive AGB ejecta. Only the Na-rich, Mg-poor giant S1673 is out of any qualitative interpretation, as the sodium survival is at variance with the strong Mg burning and Si production. We predict that the oxygen abundance in the stars with low Mg of NGC 2419 must be extremely low.

3.1. Understanding K production in the HBB phase

Mucciarelli et al. (2012) discovered the presence of two distinct, well separated populations in NGC 2419, differing in their magnesium and potassium contents, with the Mg-poor population significantly enriched in potassium, by a factor ~ 10 . In Fig. 2 we plot their data together with the data by Cohen & Kirby (2012) that confirm the K-dichotomy. Notice that also in this plot the giant pinned up as a (black) triangle is very rich in K, confirming the advanced nucleosynthesis (and the difficulty in explaining the high sodium).

Potassium is produced by proton capture on the argon nuclei. The reactions involved start from ^{36}Ar , an α -nucleus that will be the most abundant form of argon at so low metallicities, as shown by models of galactic chemical evolution (Timmes et al. 1995; Kobayashi et al. 2011). The chain is $^{36}\text{Ar}(p,\gamma)^{37}\text{K}(e^+,\nu)^{37}\text{Cl}(p,\gamma)^{38}\text{Ar}(p,\gamma)^{39}\text{K}$. We checked the relevant cross sections by means of the NETGEN tool (Aikawa et al. 2005): all of them increase by orders of magnitude at temperature above 10^8K , so that the details of the envelope structure of our AGB and SAGB models can be relevant to achieve or not the required nucleosynthesis. In order to reach the K production, we had to increase the cross section $^{38}\text{Ar}(p,\gamma)^{39}\text{K}$ by a factor 100, but also a stronger HBB, leading to temperatures at the base of the envelope exceeding $\sim 150\text{MK}$, can achieve a similar result. As the initial argon largely exceeds the initial potassium content, even a soft activation of the Ar-burning reactions may favor a great increase in the potassium

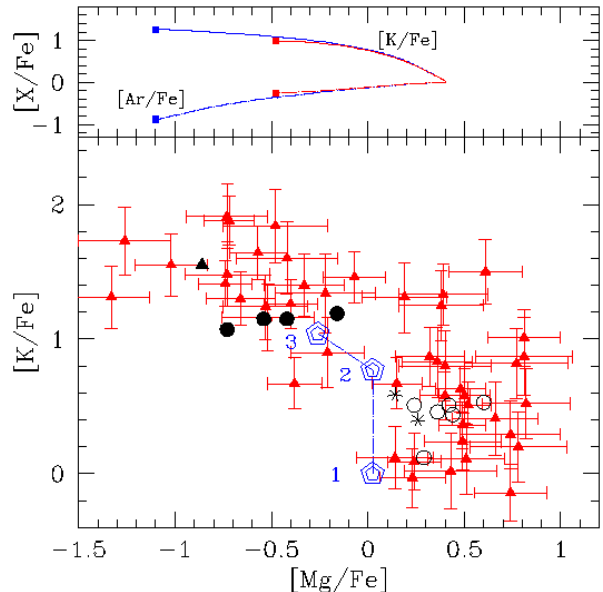


FIG. 2.— The Mg–K data by Mucciarelli et al. (2012) (red triangles with error bars) and Cohen & Kirby (2012) (symbols as in Fig. 1) are compared with the yields obtained by evolving the $6 M_{\odot}$ star in three different cases: 1: with standard $^{38}\text{Ar}(p,\gamma)^{39}\text{K}$ cross section; 2: cross section increased by a factor 100; 3: cross section as in (2), and mass loss rate reduced to $1/4$. The top panel shows the run of $[K/Fe]$ and $[Ar/Fe]$ versus $[Mg/Fe]$ during the evolution in case 2 and 3. We show for each element the logarithm of the ratio of the mass fraction to the assumed initial value.

abundance. The result of exploratory evolution of the $6 M_{\odot}$ can be seen in the top panel of Fig. 2, where the increase in the surface ^{39}K , and the concomitant ^{38}Ar burning, are shown as a function of $[Mg/Fe]$ for the standard track with increased cross section, and for the speculative case in which the mass loss rate is reduced to $1/4$ of the standard rate. In this latter case, Mg reduction and K production are maximized. The main panel of Fig. 2 shows the Mg and K abundances in the sample by Mucciarelli et al. (2012) and in the Cohen & Kirby (2012) sample. The double pentagons show the yields of the $6 M_{\odot}$ evolution, (1) in the standard case (unchanged cross sections), (2) in the case of increased cross section, and (3) in the case of increased cross section and reduced mass loss. The models show that this path is worth a more complete exploration.

We have discussed so far only the elemental abundances in Cohen & Kirby (2012) for which HBB provides a possible nucleosynthesis path. Nevertheless, it is necessary to touch the problem of Calcium. Cohen et al. (2010, 2011) found larger Ca abundances in their Mg-poor sample. Mucciarelli et al. (2012) questioned whether the difference in abundance could be attributed to the different atmospheric structure, in the presence of such Mg differences, but Cohen & Kirby (2012) discuss in depth that this can not be the case. So we must accept the Ca variations. Where do these variations come from? At low metallicity, SN ejecta contain more α -elements than iron (Kobayashi et al. 2006), a result dependent on the assumptions made on the mass cut (e.g. Limongi & Chieffi 2003). A small contamination from SN ejecta could then be a viable solution to the calcium

problem, although a detailed model should be worked out to see whether this is feasible maintaining the lack of iron variations and the magnesium depletion. Alternatively, we stretch our results and leave this problem open, by asking whether the same p-capture chains could reach ^{40}Ca from ^{39}K .

4. CONCLUSIONS

The abundances of light elements observed in NGC 2419 have been compared to the chemical patterns expected for SAGB and massive AGB evolving through HBB and mass loss, and having the low metallicity of this cluster. We compare directly the yields with observations, following the idea that the SG stars in this cluster are born directly from SAGB plus massive AGB ejecta (Di Criscienzo et al. 2011a). The low metallicity of the models allows a very strong HBB, especially for masses around $6M_{\odot}$, at the edge between the AGB and the SAGB regime. These ejecta are thus predicted to

produce the most extreme contamination, with a strong depletion of oxygen, a significant reduction of the initial magnesium, and only a modest increase in sodium. The models are compatible with the abundance trends in NGC 2419. The presence of a K-rich population of Mg-poor stars in this cluster is a signature of extreme nucleosynthesis, and we have shown that potassium can be produced by proton capture on Argon nuclei, if the relevant cross section is higher (by a factor 100) than the standard rate.

The results should be tested by a more detailed spectroscopic investigation. Confirming that the Mg-poor stars are extremely depleted in O, and have normal Na would support our model.

We thank Marco Limongi for useful discussion. This work has been supported by PRIN-INAF 2011: Multiple populations in Globular Clusters: their role in the Galaxy assembly (P.I. E. Carretta). E.V. was supported in part by grant NASA-NNX10AD86G.

REFERENCES

- Aikawa M., Arnould M., Goriely S., Jorissen A., Takahashi K., 2005, *A&A*, 411, 1195
- Blöcker T., 1995, *A&A*, 297, 727
- Blöcker T., Schönberner D., 1991, *A&A*, 244, L43
- Caloi V., D’Antona F. 2005, *A&A*, 435, 987 Caloi, V. & D’Antona, F. 2007, *A&A*, 463, 949
- Canuto V., Mazzitelli I. 1991, *ApJ*, 370, 295 Gratton, R., & Lucatello, S. 2009, *A&A*, 505, 139
- Cohen, J. G., Kirby, E. N., Simon, J. D., & Geha, M. 2010, *ApJ*, 725, 288
- Cohen, J. G., Huang, W., & Kirby, E. N. 2011, *ApJ*, 740, 60
- Cohen, J. G., & Kirby, E. N. 2012, *arXiv:1209.2705*
- Cottrell P. L., Da Costa G. S. 1983, *ApJ*, 245, L79
- D’Antona F., Bellazzini M., Caloi V., Fusi Pecci F., Galletti S., Rood R. T. 2005, *ApJ*, 631, 868
- D’Antona, F., Caloi, V., Montalbán, J., Ventura, P., & Gratton, R. 2002, *A&A*, 395, 69
- D’Antona F., & Caloi V. 2004, *ApJ*, 611, 871
- Decressin T., Meynet G., Charbonnel C., Prantzos N., & Ekström S. 2007a, *A&A*, 464, 1029
- Decressin T., Charbonnel C., & Meynet G. 2007b, *A&A*, 475, 859
- D’Ercole, A., Vesperini E., D’Antona F., McMillan S. L. W., & Recchi S. 2008, *MNRAS*, 391, 825
- D’Ercole A., D’Antona F., Ventura P., Vesperini E., & McMillan S. L. W. 2010, *MNRAS*, 407, 854
- D’Ercole A., et al. 2012, *MNRAS*, 423, 1521
- De Mink S. E., Pols O. R., Langer R. G. 2009, *MNRAS*, 507, L1
- Di Criscienzo M., D’Antona F., Milone A. P., Ventura P., Caloi V., Carini R., D’Ercole, A., Vesperini E., Piotto, G. 2011a, *MNRAS*, 414, 3381
- Di Criscienzo M., Greco C., Ripepi V., Clementini G., Dall’Ora M., Marconi M., Musella I., Federici L., Di Fabrizio L. 2011b, *AJ*, 141, 81
- Fenner, Y., Campbell, S., Karakas, A. I., Lattanzio, J. C., & Gibson, B. K. 2004, *MNRAS*, 353, 789
- Gratton, R. G., & Carretta, E. 2010, *A&A*, 521, A54
- Gratton R. G., Carretta E., Bragaglia A., 2012, *ARA&A*, 20, 50
- Herwig F. 2004, *ApJ*, 605, 425
- Karakas, A. I., & Lattanzio, J. C. 2003, *Pub. Astron. Soc. Australia*, 20, 279
- Karakas, A. I. 2010, *MNRAS*, 403, 1413
- Karakas, A. I., García-Hernández, D. A., & Lugaro, M. 2012, *ApJ*, 751, 8
- Kobayashi, C., Umeda, H., Nomoto, K., Tominaga, N., & Ohkubo, T. 2006, *ApJ*, 653, 1145
- Kobayashi, C., Karakas, A. I., & Umeda, H. 2011, *MNRAS*, 414, 3231
- Layden A. C., Ritter L. A., Welch D. L., & Webb T. M. A. 1999, *AJ*, 117, 1313
- Limongi, M., & Chieffi, A. 2003, *ApJ*, 592, 404
- Lugaro, M., Karakas, A. I., Stancliffe, R. J., & Rijs, C. 2012, *ApJ*, 747, 2
- Milone A. P., Piotto G., King I. R., et al. 2010, *ApJ*, 709, 1183
- Milone A. P., Marino, A. F., Piotto G., Bedin L. R., Anderson J., Aparicio A., Cassisi S., Rich R. M., 2012, *ApJ*, 745, 27
- Mucciarelli A., Bellazzini M., Ibata R., Merle T., Chapman S. C., D’Alessandro E., Sollima A. 2012, *Astroph J* 1208.0195v1
- Norris J. E. 2004, *ApJ Letters*, 612, L25
- Piotto G., et al. 2007, *ApJ Letters*, 661, L53
- Prantzos N., Charbonnel C., Iliadis C. 2007, *A&A*, 470, 179
- Pumo L., D’Antona F., Ventura P. 2008, *ApJ*, 672, 25
- Ripepi V., et al. 2007, *ApJ*, 667, L61
- Siess L. 2010, *A&A*, 512, A10
- Snedden C., Kraft R. P., Shetrone M. D., Smith G. H., Langer G. E., Prosser C. F. 1997, *AJ*, 114, 1964
- Stancliffe R.J., Tout C.A., Pols O.R. 2004, *MNRAS*, 352, 984
- Timmes F. X., Woosley S. E., Weaver T. A. 1995, *ApJS*, 98, 61
- Ventura P., D’Antona F., Mazzitelli I., & Gratton R. 2001, *ApJ*, 550, L65
- Ventura P., D’Antona F., & Mazzitelli I. 2002, *A&A*, 393, 215
- Ventura P., D’Antona F., 2005, *A&A*, 341, 279
- Ventura P., D’Antona F., 2009, *A&A*, 499, 835
- Ventura P., Carini R., & D’Antona F. 2012, *MNRAS*, 411, 3865
- Ventura P., & D’Antona F. 2011, *MNRAS*, 410, 2760